Full paper/Mémoire

# Porphyrins fused to *N*-heterocyclic carbene palladium complexes as tunable precatalysts in Mizoroki–Heck reactions: How the porphyrin can modulate the apparent catalytic activity?

## Complexes de palladium de carbènes N-hétérocycliques fusionnés à des porphyrines comme pré-catalyseurs modulables de la réaction de Mizoroki–Heck : Comment la porphyrine peut-elle moduler l'activité catalytique apparente?

Jean-François Lefebvre, Jean-François Longevial, Karine Molvinger, Sébastien Clément, Sébastien Richeter[*]

*Université de Montpellier, Institut Charles Gerhardt — UMR 5253, Campus Triolet, CC1701, Place Eugène Bataillon, 34095 Montpellier Cedex 5, France*

### A R T I C L E   I N F O

### A B S T R A C T

Porphyrins fused to *N*-heterocyclic carbenes (NHCs) **1M**, with inner metal M = Ni, Cu, Zn and H2, were used to synthesize palladium(II) complexes. These complexes behaved as precatalysts for high-temperature Mizoroki–Heck reactions between iodobenzene and styrene. Despite similar electronic properties between **1M** ligands, catalytic activity was found to significantly depend on the presence, or not, of a central metal incorporated in the porphyrin core: a conversion of iodobenzene between 80–90% was observed with metalloporphyrins (M = Ni, Cu and Zn), whereas only 30% was observed with free-base porphyrins (M = H2) after 10 h. Palladium leaching and subsequent trapping of free palladium in the inner core of the free-base porphyrin modified the concentration of Pd(0) active species and may explain the lower catalytic activity observed.

© 2015 Académie des sciences. Published by Elsevier Masson SAS. This is an open access article under the CC BY-NC-ND license (http://creativecommons.org/licenses/by-nc-nd/4.0/).

### R É S U M É

Des porphyrines conjuguées à des carbènes *N*-hétérocycliques **1M** avec M = Ni, Cu, Zn et H2 ont été utilisées pour synthétiser des complexes de palladium(II). Ces complexes sont des pré-catalyseurs de la réaction de couplage de Heck entre l'iodobenzène et le styrène à haute température. Malgré des propriétés électroniques similaires entre les ligands **1M**, les activités catalytiques dépendent significativement de la présence, ou non, d'un métal central dans la porphyrine : une conversion de 80–90% de l'iodobenzène est observée avec les

* Corresponding author.
  *E-mail address:* srichter@univ-montp2.fr (S. Richeter).

métalloporphyrines (M = Ni, Cu et Zn), tandis qu'une conversion de seulement 30% est observée avec des porphyrines bases libres (M = H2) après 10 heures de réaction. La libération de palladium et son piégeage dans la porphyrine base libre modifie la concentration d'espèces actives de Pd(0) et peut expliquer la plus faible activité catalytique observée.

## 1. Introduction

Incorporation of additional coordination sites within the backbone of a ligand coordinated to a catalytic site potentially allows the catalytic activity to be modulated through the complexation of metal cations. Allosteric effects [1] and/or electronic effects [2] may be implicated to explain the modulation of the catalytic activity observed. Porphyrins bearing peripheral coordination site(s) are interesting scaffolds to investigate how it is possible to tune the electronic and catalytic properties of the outer metal(s) thanks to the inner metal (or *vice versa*) [2–5]. For example, Osuka and co-workers reported the synthesis of metalloporphyrins bearing external N–C–N pincer type Pd[II] complexes, which exhibited markedly different catalytic activities in typical Mizoroki−Heck reactions depending on the inner metals [3]. Although the mechanism of the present Mizoroki−Heck system is unclear, it is known that nearly all Pd precatalysts slowly decompose at high temperatures (> 120 °C),[6] *i.e.* temperatures typically used in Mizoroki−Heck reactions, to liberate soluble "*ligand-free*" palladium colloids or nanoparticles [7]. It has also been shown for other metalloporphyrins bearing external Pd[II] complexes that the porphyrin plays a crucial role in the apparent catalytic activity of the Pd-precatalysts. More exactly, the nature of the inner metal strongly modulates the release of adequate amounts of active Pd[0] species in high-temperature Mizoroki−Heck reaction mixtures [2,4,7]. In the course of our studies, we were interested in the synthesis of metalloporphyrins annulated to peripheral *N*-heterocyclic carbenes (NHCs, Scheme 1)
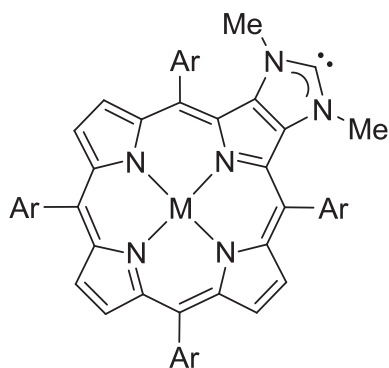
[8]. *N*-heterocyclic carbenes (NHCs) have become an important class of ligands in the field of catalysis, since they can form very stable bonds with a wide range of transition-metals in low and high oxidation states [9]. Recently, we showed that porphyrin-NHCs scaffolds **1M** (Scheme 1, M = Ni, Cu, Zn and H2) provide an interesting way to remote the electronic properties of NHC by varying the inner metal of the porphyrin [10] and to build multiporphyrinic systems to investigate energy transfer processes between chromophores [11]. Here, we present the use of palladium complexes bearing porphyrin-NHCs as precatalysts in the Mizoroki−Heck reaction. We notably demonstrate how the porphyrin core and its inner metal can affect the apparent catalyst activity in the course of the Mizoroki−Heck reaction. Similar to previous reports, mercury poisoning tests and transmission electronic microscopy (TEM) studies suggest that these complexes may readily form Pd nanoparticles at elevated temperature [7].

## 2. Results and discussion

### 2.1. Electronic properties of porphyrin-NHCs

Imidazolium salts **2M** were obtained in good yields starting from *meso*-tetra(4-*tert*-butylphenyl)porphyrin, and were characterized by using conventional techniques (Scheme 2) [12]. To evaluate the electron-donating ability of the porphyrin ring, we studied the electrochemical oxidation processes of **2M** by cyclic voltammetry (CV) and rotating disk voltammetry (RDV) in $CH_2Cl_2$ with $Bu_4NPF_6$ as the supporting electrolyte: the first oxidation potentials ($E_{OX1}$ *vs* Fc/Fc$^+$) are shifted anodically in the order of **2Zn** (+0.36 V) < **2Cu** (+0.54 V) < **2H2** (+0.57 V) < **2Ni** (+0.64 V). Thus, the electron donating ability of the porphyrin ring increases in the order of **2Ni** < **2H2** ≤ **2Cu** < **2Zn**. To quantify the electron-donor ability of the corresponding carbene ligand, we synthesized the corresponding *cis*-[(**1M**) Rh(CO)$_2$Cl] complexes and measured their CO-stretching frequencies to study the influence of the inner metal of the porphyrin on the electronic properties of the outer NHC ligand [10,13]. After obtaining the imidazolium salts of **3M** by reacting **2M** with AgBF$_4$ in acetonitrile, the rhodium(I) complexes **4M** were obtained by the *in situ* deprotonation of **3M** in the presence of [{Rh(COD)Cl}$_2$] (Scheme 2). Then, complexes **5M** were obtained by bubbling carbon monoxide through a solution of complexes **4M** in $CH_2Cl_2$ (Scheme 2). Two CO stretching frequencies were observed by IR spectroscopy confirming the *cis* geometry of all complexes **5M**. Similar average CO stretching vibrations were observed at 2040.5, 2041, 2041 and 2041.5 cm$^{-1}$, respectively, for **5Zn**, **5Cu**, **5H2** and **5Ni**. These data clearly show that NHCs **1M** with M = H2 and M = divalent metal cations



**1M**

Ar = 4-*t*BuPh
M = Ni, Cu, Zn or H2

**Scheme 1.** Structure of the porphyrin-NHC scaffold **1M**.
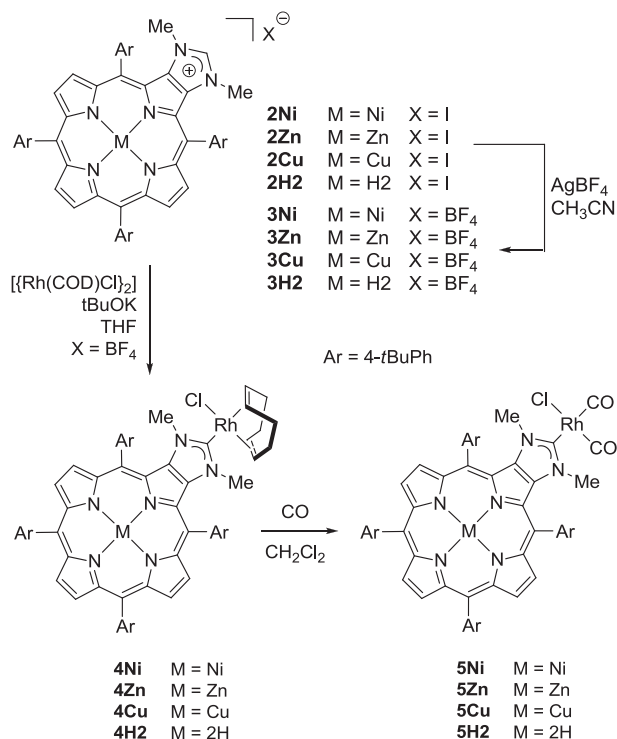
**Scheme 2.** Structures of compounds **2M**–**5M**.

such as Ni$^{II}$, Cu$^{II}$ and Zn$^{II}$ display very similar electron-donor abilities. It is also noticeable that the σ-donor ability of the NHCs is poorly influenced by the π-electron-donor ability of the porphyrin ring.

### 2.2. Synthesis of palladium(II) complexes **6M** and **7M**

To investigate the effects of the inner metal of the porphyrin core on the catalytic activity of a metal anchored at the periphery of the porphyrin, we synthesized palladium complexes containing porphyrin-NHCs **1M** as ancillary ligands [8,11]. The reaction of the imidazolium salts **2M** with 0.5 equivalent of Pd(OAc)$_2$ in refluxing THF afforded a mixture of two complexes after standard workup and crystallization. No remaining imidazolium salt was observed in the reaction mixtures after two hours. The two complexes formed in the course of the complexation reactions are *trans*-[PdI$_2$(**1M**)$_2$] and [{PdI($\mu$-I)(**1M**)}$_2$], respectively, labeled **6M** and **7M** (Scheme 3). They were obtained in a **6M**/**7M** ratio of ~4:1 and similar results were obtained with M = Ni, Cu, Zn or H2 showing that the inner metal has no influence on the **6M**/**7M** ratio. The two complexes **6M** and **7M** could be separated by column chromatography on silica gel.
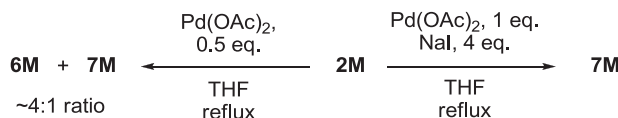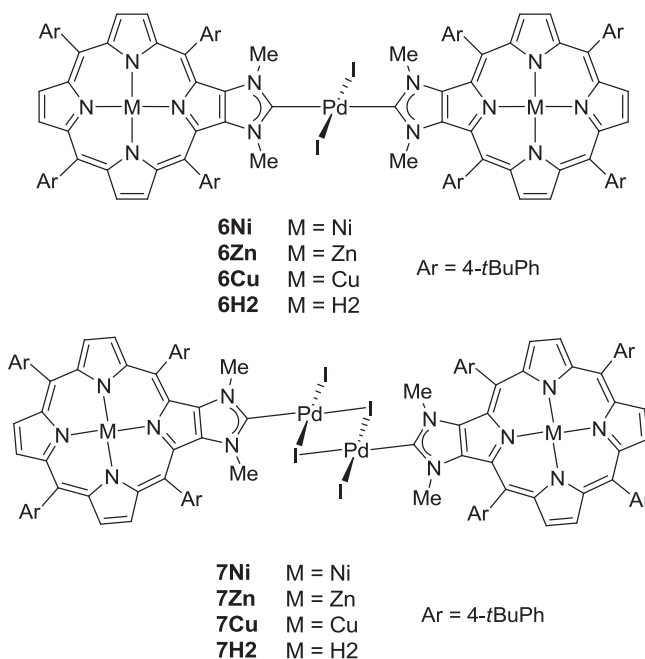
No signal corresponding to the iminium proton could be observed in the $^1$H NMR spectra of *trans*-[PdI$_2$(**1M**)$_2$] complexes, confirming the formation of the NHC–Pd bonds. Their parent mass ion peaks could be observed by ESI-TOF mass spectrometry: for example $m/z = 2175.7$ for **6H2** (calcd for (C$_{126}$H$_{135}$I$_2$N$_{12}$Pd)$^+$ = 2175.8 [(M+H)$^+$]). $^1$H NMR spectroscopy also showed the 2-fold symmetry of **6M**

complexes. The *trans* geometry around the Pd$^{II}$ was only confirmed by X-ray diffraction analysis for **6Ni**, because no suitable monocrystals for X-ray diffraction analysis were obtained for other complexes **6M** [8]. However, we observed that **6Ni** could be also obtained by reacting **6H2** with Ni(acac)$_2$ and this experiment indirectly showed the *trans* geometry around the Pd$^{II}$ of **6H2**. Knowing that **6H2** has a Pd$^{II}$ center with a *trans* geometry and that metallation reactions with Zn(OAc)$_2$ and Cu(OAc)$_2$ afforded respectively **6Zn** and **6Cu**, we presume that Pd$^{II}$ centers of **6Zn** and **6Cu** have a *trans* geometry too [11]. Herrmann and co-workers showed that *cis*-[PdI$_2$(NHC)$_2$] complexes could be obtained by reacting N,N′-dimethylimidazolium salts with Pd(OAc)$_2$ in refluxing THF.[14] *Cis* isomers are usually obtained with small N-substituting groups such as methyl groups, and *trans* isomers are obtained with bulky N-substituting groups. In our case, the NHC precursors of **1M** are also N,N′-dimethylimidazolium salts, but we did not observe the formation of *cis*-[PdI$_2$(**1M**)$_2$] isomers, which are presumably energetically unfavored [11].

To avoid the formation of a mixture between *trans*-[PdI$_2$(**1M**)$_2$] and [{PdI($\mu$-I)(**1M**)}$_2$] complexes, we used the classical conditions for the synthesis of dimeric mono-coordinated [{PdI($\mu$-I)(NHC)}$_2$] complexes, *i.e.* addition of 1 equiv of Pd(OAc)$_2$ and NaI in excess to a solution of **2M** in THF (Scheme 3). Following this procedure, complexes **7M** were obtained in good yields (83% yield for **7H2**, see reference [11]). Mass spectrometry analyses were performed for these complexes. The parent mass ion peak of **7H2** could be observed at $m/z = 2537.5$ (calcd for (C$_{126}$H$_{135}$I$_4$N$_{12}$Pd$_2$)$^+$ = 2537.52 [(M+H)$^+$]) in its ESI-TOF mass spectrum, but parent mass ion peaks of the complexes including metallopoporphyrins **7M** (M = Ni, Cu, Zn) could not be detected and only fragments were observed. The $^1$H NMR spectra of the complexes **7M** are similar to those of the *trans* isomers **6M** except some signals for the protons of the two *meso* aryl groups of **7M** which were broad and split at room temperature and sharper at higher temperature. Variable temperature $^1$H NMR experiments confirmed the dynamic nature of this phenomenon.[11] This is consistent with the perpendicular orientation of each porphyrin mean plane with respect to the Pd$_2$($\mu$-I)$_2$ bridge in complexes **7M**, the slower rotation of the *meso* aryl groups at room temperature, and thus, different chemical environments for the protons close to the Pd$_2$($\mu$-I)$_2$ unit. Energy-dispersive X-ray (EDX) analyses appeared also to be an interesting tool to characterize complexes **6M** and **7M** (M = Ni, Cu or Zn) since different M/Pd/I chemical compositions were expected for these two families (Table 1). EDX analyses of complexes **7M** showed chemical compositions of M/Pd/I in *ca.* 1:1:2 ratios in accordance with the [{PdI($\mu$-I)(**1M**)}$_2$] structures proposed for these complexes. Chemical compositions of M/Pd/I in *ca.* 2:1:2 ratios were observed for **6M** confirming that one palladium cation was coordinated by two **1M** ligands and two iodides.

### 2.3. Mizoroki–Heck coupling reactions with **7M** used as precatalysts

Knowing that complexes **6M** were only poorly soluble in DMF, we used complexes **7M** as precatalysts for the

**6Ni**  M = Ni
**6Zn**  M = Zn
**6Cu**  M = Cu
**6H2**  M = H2

Ar = 4-*t*BuPh

**7Ni**  M = Ni
**7Zn**  M = Zn
**7Cu**  M = Cu
**7H2**  M = H2

Ar = 4-*t*BuPh

$$\textbf{6M} + \textbf{7M} \xleftarrow[\text{reflux}]{\substack{\text{Pd(OAc)}_2, \\ 0.5 \text{ eq.} \\ \text{THF}}} \textbf{2M} \xrightarrow[\text{reflux}]{\substack{\text{Pd(OAc)}_2, 1 \text{ eq.} \\ \text{NaI, 4 eq.} \\ \text{THF}}} \textbf{7M}$$

~4:1 ratio

**Scheme 3.** Synthesis of complexes **6M** and **7M**.

Mizoroki–Heck coupling reaction between iodobenzene and styrene. The catalytic experiments were conducted in DMF at 120 °C with 1 equiv. of iodobenzene, 1.1 equiv. of styrene, 2 equiv. of diisopropylethylamine, and 0.04 mol% of the precatalyst **7M**, *i.e.* 0.08 mol% of [Pd]. The reaction progress was monitored by gas chromatography and ^{1}H NMR spectroscopy. We have previously shown that **1M** ligands with M = Ni, Cu, Zn and H2 display very similar electron-donor abilities. They also exhibit identical steric properties, since no modification has been brought to the organic backbone. Knowing that, it was reasonable to anticipate that reaction profiles obtained for Mizoroki–Heck reactions catalyzed by the four **7M** precatalysts should be similar.

Reaction profiles (*i.e.* conversion of iodobenzene *vs.* time) at one hour intervals are displayed in Fig. 1. ^{1}H NMR studies confirmed that styrene was converted to *trans*-stilbene. At 0.04 mol % of the precatalyst **7M**, conversions of 80–90% were reached by **7Zn**, **7Ni** and **7Cu** after 10 h. No significant induction period was observed for **7Cu**, the most active pre-catalyst in the early stage of the reaction. Sigmoidal curves could be observed for the conversion of iodobenzene for **7Ni** and **7Zn**. These induction times are commonly observed for high-temperature Mizoroki–Heck reactions using NHC-Pd[II] precatalysts, and it was proposed that during this period, catalytically active Pd[0] species are formed and enter catalytic cycles. UV-visible spectroscopy was performed in the course of the Mizoroki–Heck

reactions catalyzed by complexes **7M**, and the case of **7Zn** is represented in Fig. 2a as an example. Data obtained indicate that metalloporphyrins did not decompose in the course of the reactions and, more importantly, remained metallated. For example, the Soret band of **7Zn** was only slightly red-shifted (~1–2 nm) and Q bands remained at similar positions (Fig. 2a).

Surprisingly, the precatalyst **7H2** appeared to be significantly less active and a conversion of only 30% was reached after 10 h (Fig. 1). To ascertain if the incorporation of the inner metal in the porphyrin core was able to

**Table 1**
Energy-dispersive X-ray (EDX) analyses of **6M** and **7M**.[a]

| | % atomic[b] | | |
| --- | --- | --- | --- |
| | M | Pd | I |
| **6Ni**[c] | 34.9 (3.0) | 22.0 (1.7) | 43.1 (2.1) |
| **6Cu**[d] | 40.8 (8.2) | 20.0 (3.1) | 39.2 (5.8) |
| **6Zn**[e] | 38.9 (1.7) | 21.3 (1.1) | 39.8 (0.6) |
| **7Ni**[c] | 24.9 (1.4) | 26.7 (1.2) | 49.3 (2.5) |
| **7Cu**[d] | 27.8 (3.6) | 26.2 (1.3) | 46.0 (3.8) |
| **7Zn**[e] | 26.0 (1.9) | 26.9 (1.2) | 47.1 (0.8) |

[a] Mean normalized values obtained for four different spectra. Values indicated in parentheses correspond to the standard deviations.
[b] Theoretical % atomic values calculated for **6M** and **7M** (M = Ni, Cu or Zn) are, respectively, M/Pd/I 40:20:40 and 25:25:50.
[c] Normalized for Ni, Pd and I elements.
[d] Normalized for Cu, Pd and I elements.
[e] Normalized for Zn, Pd and I elements.

increase catalytic activity, the Mizoroki–Heck reaction catalyzed by **7H2** was performed and an excess of zinc(II) acetate monohydrate was added to the reaction mixture after two hours (Fig. 3a). We observed that the catalytic activity increased immediately and this could be correlated with the metallation of the inner core of the porphyrin by $Zn^{II}$ by analyzing aliquots of the reaction mixture using UV-visible spectroscopy. For the Mizoroki–Heck reaction catalyzed by **7H2**, the four Q bands of the free-base porphyrin were observed before the addition of $Zn(OAc)_2$ (Fig. 3b, dotted line). However, the fourth Q band at low energy completely vanished 30 min after the addition of $Zn(OAc)_2$ as a consequence of the metallation of the inner core of the porphyrin with $Zn^{II}$ (Fig. 3b, dashed line). This experiment confirmed that the increased catalytic activity observed after the addition of $Zn(OAc)_2$ could be correlated with the metallation of the inner core of the porphyrin with $Zn^{II}$. This begs the question, "why is the precatalyst **7H2** less active compared to **7M** (M = Ni, Cu, Zn) despite the fact that the corresponding NHCs **1M** exhibit identical steric and quite similar electronic properties?"

To answer this question, UV-visible spectroscopy was performed in the course of the reaction catalyzed by **7H2** and significant changes occurred in the Q band regions, notably, the Q band at ~660 nm which slowly vanished during the course of the reaction (Fig. 2b). Knowing that several studies reported that NHC-Pd complexes decomposed in the course of high-temperature Mizoroki–Heck reactions,[6,7] we attributed this spectral evolution to the
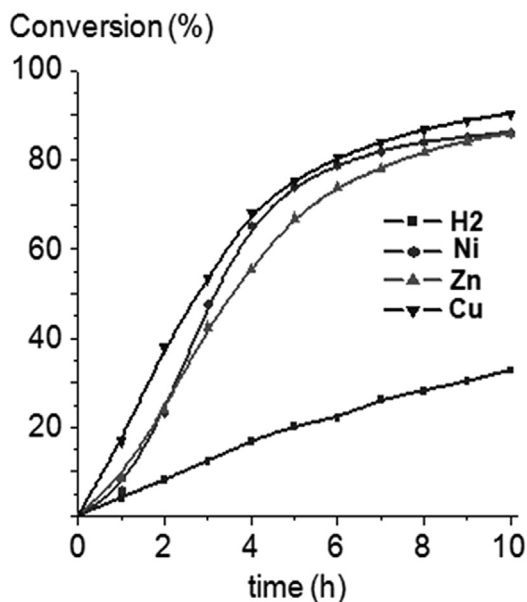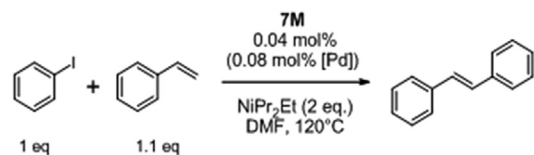
metallation of the free-base porphyrin cores with leached palladium issued from the decomposition of precatalyst **7H2**. To verify this hypothesis, we added an excess of tri-fluoroacetic acid to aliquots of the reaction mixture at different times (Fig. 4). When TFA is added to aliquots of the reaction mixture after 10 min, a change of color from purple to green occurred due to the protonation of the free-base porphyrin derivatives. This was further confirmed by UV-visible spectroscopy: the Soret band was bath-ochromically shifted from 429 to 455 nm and one intense Q band appeared at 676 nm (Fig. 4a,b) [10a]. When TFA was added to aliquots of the reaction mixture after four hours, two kinds of porphyrin derivatives could be observed (Fig. 4c): protonated porphyrin derivatives (Soret band and Q band, respectively, at 455 and 676 nm) and $Pd^{II}$-porphyrin derivatives (Soret band at 425 nm; TFA alone is not able to remove $Pd^{II}$ from the inner core of the porphyrin). According to these data, the progressive metallation of the inner core of porphyrin during the reaction



**Fig. 1.** Time-profile of the Mizoroki–Heck reaction with **7M** used as pre-catalysts: conversion of iodobenzene *vs.* reaction time.
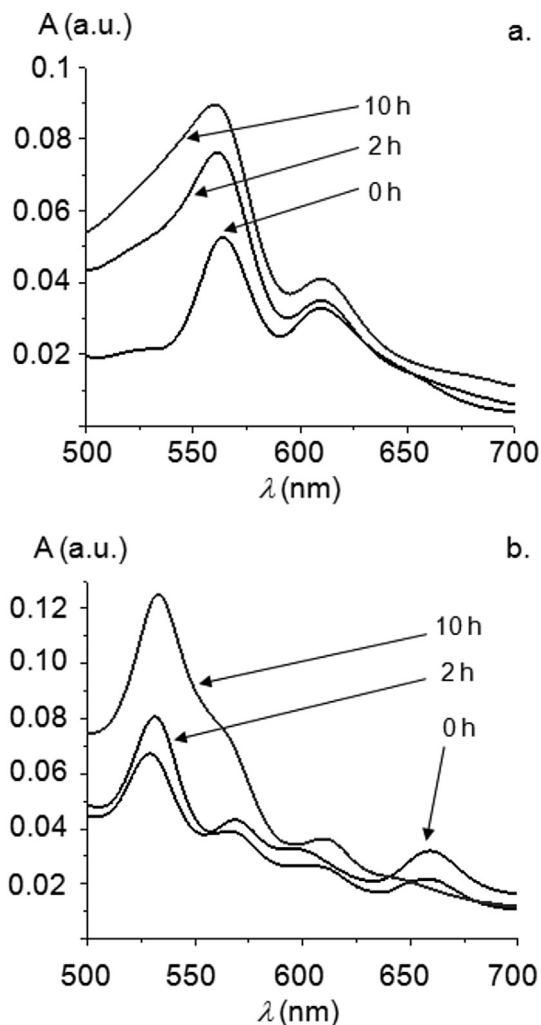


**Fig. 2.** (a) Evolution of the Q bands during Mizoroki–Heck reactions (Soret band normalized at A = 1) catalyzed by **7Zn**. (b) Evolution of the Q bands during Mizoroki–Heck reactions (Soret band normalized at A = 1) catalyzed by **7H2**.

with Pd$^{II}$ was obvious. We assume that all Mizoroki–Heck reactions catalyzed by **7M** (M = H2, Ni, Cu, Zn) release palladium in a similar manner, because they exhibit identical steric and quite similar electronic properties.

To identify more accurately the porphyrin derivatives generated in the reaction mixtures, mass spectrometry (ESI-TOF MS, positive mode) was performed after 10 h (See Supporting Information, Figs. S1 and S2). For the Mizoroki–Heck reaction catalyzed by **7Ni**, we identified Ni$^{II}$ complexes **2Ni** and **8Ni** (Scheme 4). We presume that compounds **8M** with a phenyl ring at the C(2') position could be obtained in the course of the Mizoroki–Heck reaction through a reductive elimination of Pd$^{II}$ affording Pd$^0$ species which are catalytically active (Scheme 4). For the Mizoroki–Heck reaction catalyzed by **7H2**, we identified by mass spectrometry the Pd complexes **2Pd** (imidazolium salt



**Fig. 3.** (a) Time-profile of the Mizoroki–Heck reaction with **7H2** used as the precatalyst: zinc(II) acetate monohydrate added (200 equiv *vs* **7H2**) after two hours. (b) Evolution of the Q bands during Mizoroki–Heck reactions (Soret band normalized A = 1) catalyzed by **7H2** + 200 equiv of Zn(OAc)$_2$ after 2 h.

**2M** with M = Pd) and **8Pd**, and the corresponding free-base **2H2** and **8H2**. Thus, it is quite obvious that in the case of the Mizoroki–Heck reaction catalyzed by **7H2**, Pd leached in the course of the reaction can be *trapped* by the porphyrin cores. This phenomenon is expected to dramatically change the concentration of *free* palladium in the reaction mixture (reduction of the concentration was expected in the present case) compared to reactions catalyzed by **7M** with M = Cu, Ni and Zn. It also explains why a significant increase of the catalytic activity was observed upon metallation of the free-base porphyrin with zinc(II) in the course of the Mizoroki–Heck reaction, since leached palladium could not be trapped anymore by the porphyrin cores.

Knowing that the previously reported Pd-NHC pre-catalysts used in C–C coupling reactions such as Heck reactions decomposed to Pd nanoparticles [7], we therefore attempted to detect the presence of heterogeneous Pd. First, it should be outlined that the formation of black palladium was not observed during the reaction. Then, we performed mercury poisoning experiments by exposing reaction mixtures to an excess of Hg and the subsequent catalytic activity was completely inhibited. This strongly suggests that heterogeneous Pd nanoparticles are involved in the catalytic reactions. Samples of the reaction mixtures were also analyzed by TEM and, in some cases, the formation of nanoparticles was clearly evidenced. A representative TEM image is presented in Fig. 5 and shows the presence of nanoparticles after the Mizoroki–Heck reaction catalyzed by **7H2**, confirming the results obtained from Hg poisoning experiments.

## 3. Conclusion

*N*-heterocyclic carbene ligands **1M** fused to porphyrins across two neighboring β-pyrrolic positions were used to synthesize two kinds of palladium complexes, *i.e. trans*-[PdI$_2$(**1M**)$_2$] and [{PdI(μ-I)(**1M**}$_2$] complexes, respectively, labeled **6M** and **7M**. Complexes **7M** were then used as precatalysts for Mizoroki–Heck reactions. All NHC ligands **1M** displayed similar steric and electronic properties according to IR data obtained with *cis*-[(**1M**)Rh(CO)$_2$Cl] complexes. Upon the use of complexes **7M** in the Mizoroki–Heck reaction of iodobenzene with styrene, precatalysts containing metalloporphyrin, *i.e.* **7M** with M = Ni, Cu, Zn showed quite similar catalytic activities, although some differences were observed in the course of the formation of the catalytically active species. However, the precatalyst **7H2** containing free-base porphyrins exhibited a significantly lower activity; ~30% of conversion after 10 h compared to 80–90% observed with **7M** with M = Ni, Cu and Zn. Although comparisons with other porphyrin-based precatalysts reported by Klein Gebbink [2], Osuka [3] and Matano [4] are not easy to make (palladium complexes are on *meso* positions and ligands are different), it is clear that precatalysts containing free-base porphyrins showed the lowest activity (excluding Klein Gebbink's Mn$^{III}$ complex for which the reduction of Mn also occurred in the course of the Heck reaction). With porphyrin-NHC ligands **1M** and corresponding **7M** precatalysts, we showed that Pd leaching occurred in the course of the reaction, and that leached Pd can be *trapped* by the porphyrin in the case of **7H2**. This
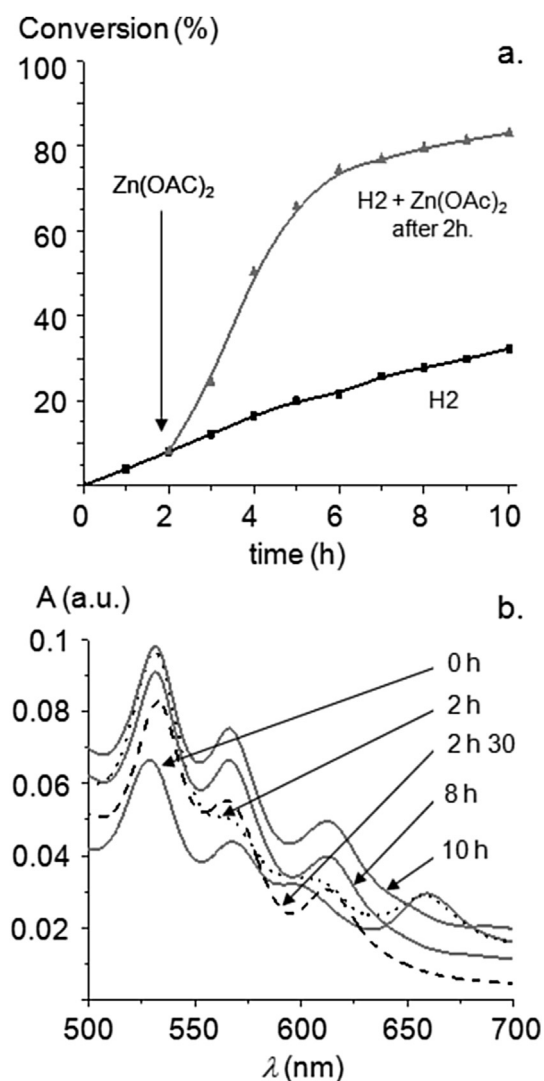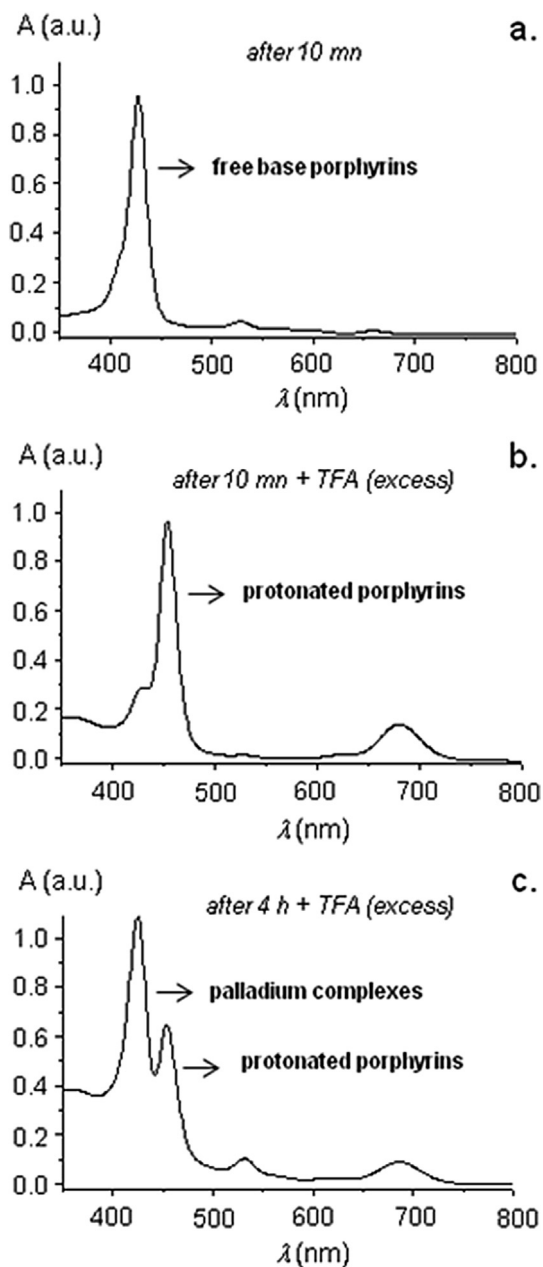
Fig. 4. UV-visible spectra of the reaction mixture during Mizoroki–Heck reaction catalyzed by **7H2**. (a) After 10 min. (b) After 10 min + TFA. (c) After 4 h + TFA.

dramatically decreased the concentration of *free* Pd available for the catalytic cycle. Moreover, poisoning experiments with Hg and TEM analyses also showed that Pd nanoparticles may play a leading role in the catalytic process in all cases. Indeed, steric and electronic properties are important factors to take into account when investigating the catalytic properties of porphyrin-based catalysts, but other important factors should also be taken into account: the metallation of the free-base porphyrin, *i.e.* incorporation of the Pd in the inner core of the porphyrin, is one of them. Other phenomena should also be taken into consideration,
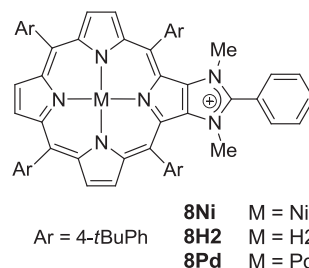


Scheme 4. Proposed structures of compounds **8M**.

such as possible aggregation of the catalysts (commonly observed with porphyrins) or possible coordination of additional ligands on the inner metal of the porphyrin. This is actually under investigation in our group.

## 4. Experimental

### 4.1. General

The synthesis of imidazolium salts **2M** and **3M** is described in references [8] and [12]. The synthesis of Rh[I] complexes **4M** and **5M** is described in reference [10]. Reactions were performed under argon using oven-dried glassware. Dry THF was obtained by distilling over $CaH_2$, and then Na/benzophenone. Preparative separations were performed by silica gel flash column chromatography (Baeckeroot-Labo 60M). Chemicals were obtained from Alfa-Aesar, Sigma-Aldrich and Acros and used as received. Reactions were monitored by thin-layer chromatography using Merck[©] TLC Silica gel 60 F254 plates. NMR spectra were recorded in $CDCl_3$ on either a Bruker 300 MHz or a 200 MHz Fourier-transform spectrometer. Chemical shifts are reported in ppm referenced to the $CHCl_3$ solvent residual peak at 7.26 ppm for [1]H. Abbreviations for ^{1}H NMR spectra used are as follows: s, singlet; d, doublet. UV-visible spectra were recorded on a Perkin Elmer Lambda 35 spectrophotometer in quartz cells. Infrared spectra were obtained in $CH_2Cl_2$ solutions in a $CaF_2$ cell with a Nicolet Avatar 320 FT-IR spectrometer. ESI mass spectra were recorded on a Q-Tof Waters 2001 MS spectrometer. MALDI-TOF mass spectra were recorded on a Bruker Ultraflex III MS spectrometer using an anthracene-1,8,9-triol matrix and PEG as the internal reference. EDX microanalyses were performed on a FEI Quanta DEG 200 environmental microscope.

### 4.2. Synthesis of Pd[II] complexes **6M** and **7M**
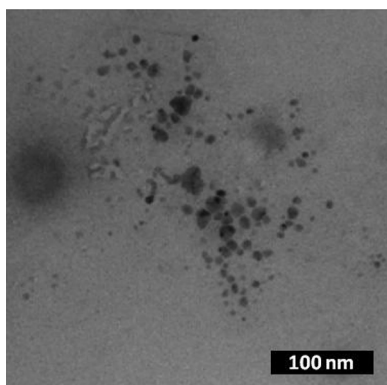
#### 4.2.1. Synthesis of complex **6H2**
The synthesis and characterization data of complex **6H2** are reported in reference [11].

#### 4.2.2. Synthesis of complex **6Ni**
The synthesis and characterization data of complex **6Ni** are reported in reference [8].

#### 4.2.3. Synthesis of complex **6Zn**
The synthesis and characterization data of complex **6Zn** were reported in reference [11].

**Fig. 5.** Transmission electronic microscopy image of the reaction mixture after the Mizoroki–Heck reaction catalyzed by **7H2**.

### 4.2.4. Synthesis of complex **6Cu**

The complex **6Cu** was synthesized following the synthetic procedure described for the synthesis of complex **6Zn** in reference [11]. UV-visible (CHCl$_3$): $\lambda_{max}$ ($\varepsilon$): 429 (546,000), 548 (39,000), and 583 nm (10,000 L.mol$^{-1}$·cm$^{-1}$). MALDI-TOF$^+$ MS: calculated for C$_{126}$H$_{128}$N$_{12}$Ni$_2$PdI$^+$: 2167.7, found: 2167.7 ([M−I]$^+$).

### 4.2.5. Synthesis of complex **7H2**

The synthesis and characterization data of complex **7H2** are reported in reference [11].

### 4.2.6. Synthesis of complex **7Ni**

The complex **7Ni** was synthesized following the synthetic procedure described for the synthesis of complex **7H2** in reference [11]. $^1$H NMR (200 MHz, 25 °C, CDCl$_3$): $\delta$ 8.74 (s, 4H, H$_{pyrrole}$), 8.70 (s, 8H, H$_{pyrrole}$), 8.10 (d broad, $^3J_{H-H} = 8.2$ Hz, 8H, H$_{Ar\ ortho}$), 7.99 (d, $^3J_{H-H} = 8.2$ Hz, 8H, H$_{Ar\ ortho}$), 7.84 (d, $^3J_{H-H} = 8.2$ Hz, 8H, H$_{Ar\ meta}$), 7.75 (d, $^3J_{H-H} = 8.2$ Hz, 8H, H$_{Ar\ meta}$), 3.41 (s, 12H, H$_{NMe}$), 1.64 (s, 36H, H$_{tBu}$), and 1.59 (s, 36H, H$_{tBu}$) ppm. $^{13}$C{$^1$H} NMR (50.3 MHz, 25 °C, CDCl$_3$): $\delta$ 167.3 (carbene), 153.1, 151.3, 144.7, 143.8, 143.3, 142.0, 138.0, 137.5, 135.4, 134.3, 133.2, 132.8, 132.7, 126.6, 125.5, 124.5, 120.8, 116.0, 38.8, 35.5, 35.3, 32.1, 32.0, 31.9, 30.1, and 1.4 ppm. UV-visible (CHCl$_3$): $\lambda_{max}$ ($\varepsilon$): 428 (542,000), 540 (36,500), 575 nm (sh 12,000 L.mol$^{-1}$·cm$^{-1}$). MALDI-TOF$^+$ MS: calculated for C$_{126}$H$_{128}$I$_3$N$_{12}$Ni$_2$Pd$_2^+$: 2517.43, found: 2517.4 ([M−I]$^+$).

### 4.2.7. Synthesis of complex **7Zn**

The complex **7Zn** was synthesized following the synthetic procedure described for the synthesis of complex **7H2** in reference [11]. $^1$H NMR (200 MHz, 25 °C, CDCl$_3$): $\delta$ 8.98 (s, 4H, H$_{pyrrole}$), 8.97 (d, $^3J_{H-H} = 5.0$ Hz, 4H, H$_{pyrrole}$), 8.86 (d, $^3J_{H-H} = 5.0$ Hz, 4H, H$_{pyrrole}$), 8.41 (d broad, $^3J_{H-H} = 8.2$ Hz, 4H, H$_{Ar\ ortho}$), 8.31 (d broad, $^3J_{H-H} = 8.2$ Hz, 4H, H$_{Ar\ ortho}$), 8.19 (d, $^3J_{H-H} = 8.2$ Hz, 8H, H$_{Ar\ ortho}$), 7.92 (d, $^3J_{H-H} = 8.2$ Hz, 8H, H$_{Ar\ meta}$), 7.81 (d, $^3J_{H-H} = 8.2$ Hz, 8H, H$_{Ar\ meta}$), 3.64 (s, 12H, H$_{NMe}$), 1.73 (s, 36H, H$_{tBu}$), and 1.66 (s, 36H, H$_{tBu}$) ppm. UV-visible (CHCl$_3$): $\lambda_{max}$ ($\varepsilon$): 433 (546,500), 561 (35,500), 605 nm (14,300 L.mol$^{-1}$·cm$^{-1}$). MALDI-TOF$^+$ MS: calculated for C$_{63}$H$_{65}$N$_6$Zn$^+$: 969.46, found : 969.47 ([M-Pd$_2$-I$_4$–**1Zn**]$^+$).

### 4.2.8. Synthesis of complex **7Cu**

The complex **7Cu** was synthesized following the synthetic procedure described for the synthesis of complex **7H2** in reference [11]. UV-visible (CHCl$_3$): $\lambda_{max}$ ($\varepsilon$): 426 (595,500), 548 (44,600), and 584 nm (sh 10,900 L.mol$^{-1}$.cm$^{-1}$). MALDI-TOF$^+$ MS: calculated for C$_{126}$H$_{128}$I$_4$N$_{12}$NaCu$_2$Pd$_2^+$: 2677.35, found: 2677.3 ([M+Na]$^+$); calculated for C$_{63}$H$_{64}$I$_2$N$_6$CuPd$^+$: 1327.17, found: 1327.1 ([M-Pd-I$_2$-**1Cu**]$^+$).

## 4.3. Heck coupling reactions between iodobenzene and styrene

### 4.3.1. Materials

Conversion percentages were determined by GC analyses performed on a Varian 3900 instrument (FID, HP5, T$_{inj}$ = 250 °C, T$_{det}$ = 275 °C, oven 75–250 °C, 20 °C.min$^{-1}$) with ethylbenzoate as internal GC standard according to the first sample ($t = 0$). The GC column was a SLB-5 MS column, length 30 m, diameter 0.25 mm. Samples for UV-visible spectroscopy (30 $\mu$L) were diluted in dichloromethane (2.97 mL).

### 4.3.2. Typical procedure

In a typical run, the precatalyst **7M** (1.7 $\mu$mol) was weighed accurately and charged in a Schlenk tube fitted with a rubber septum. The Schlenk tube was evacuated and refilled with argon. Then, anhydrous DMF (8.6 mL), ethylbenzoate (400 $\mu$L), diisopropylethylamine (1.4 mL, 8.00 mmol), styrene (460 $\mu$L, 4.50 mmol) and phenyl iodide (450 $\mu$L, 4.00 mmol) were added *via* a syringe. The reaction flask was placed into a preheated oil bath at 120 °C and the progress of the reaction was monitored by GC every hour. Coupling reactions were tested at least three times.

## Acknowledgments

## Appendix A. Supplementary data

Supplementary data related to this article can be found at http://dx.doi.org/10.1016/j.crci.2015.03.002.

## References

[1] I.O. Fritsky, R. Ott, H. Pritzkow, R. Krämer, Chem. Eur. J 7 (2001) 1221.
[2] B.M.J.M. Suijkerbuijk, S.D. Herreras Martínez, G. van Koten, R.J.M. Klein Gebbink, Organometallics 27 (2008) 534.
[3] S. Yamaguchi, T. Katoh, H. Shinokubo, A. Osuka, J. Am. Chem. Soc. 129 (2007) 6392.
[4] Y. Matano, K. Matsumoto, T. Shibano, H. Imahori, J. Porphyrins Phthalocyanines 15 (2011) 1172.
[5] R.-S. Lin, M.-R. Li, Y.-H. Liu, S.-M. Peng, S.-T. Liu, Inorg. Chim. Acta 363 (2010) 3523.
[6] (a) I.P. Beletskaya, A.V. Cheprakov, J. Organomet. Chem. 689 (2004) 4055;
(b) F. Alanso, I.P. Beletskaya, M. Yus, Tetrahedron 61 (2005) 11771;
(c) J.G. de Vries, Dalton Trans. (2006) 421;
(d) N.T.S. Phan, M. van der Sluys, C.W. Jones, Adv. Synth. Catal. 348 (2006) 609;
(e) M. Weck, C.W. Jones, Inorg. Chem. 46 (2007) 1865;

(f) A.M. Trzeciak, J.J. Ziólkowski, Coord. Chem. Rev. 249 (2007) 2308;

(g) A.M. Trzeciak, J.J. Ziólkowski, Coord. Chem. Rev. 251 (2007) 1281;

(h) R.H. Crabtree, Chem. Rev. 112 (2012) 1536.

[7] (a) H. Baier, P. Metzner, T. Körzdörfer, A. Kelling, H.-J. Holdt, Eur. J. Inorg. Chem. (2014) 2952;

(b) E.C. Keske, O.V. Zenkina, R. Wang, C.M. Crudden, Organometallics 31 (2012) 6215;

(c) Y.-C. Lin, H.-H. Hsueh, S. Kanne, L.-K. Chang, F.-C. Liu, I.J.B. Lin, G.-H. Lee, S.-M. Peng, Organometallics 32 (2013) 3859.

[8] S. Richeter, A. Hadj-Aïssa, C. Taffin, A. van der Lee, D. Leclercq, Chem. Commun. (2007) 2148.

[9] (a) W.A. Herrmann, C. Köcher, Angew. Chem. Int., Ed. Engl. 36 (1997) 2162;

(b) D. Bourissou, O. Guerret, F.P. Gabbaie, G. Bertrand, Chem. Rev. 100 (2000) 39;

(c) W.A. Herrmann, Angew. Chem., Int. Ed. 41 (2002) 1290;

(d) F. Glorius, Top. Organomet. Chem. 21 (2007) 1;

(e) E.A.B. Kantchev, C.J. O'Brien, M.G. Organ, Angew. Chem., Int. Ed. 46 (2007) 2768;

(f) S. Wuertz, F. Glorius, Acc. Chem. Res. 41 (2008) 1523;

(g) F.E. Hahn, M.C. Jahnke, Angew. Chem., Int. Ed. 47 (2008) 3122;

(h) B. Alcaide, P. Almendros, A. Luna, Chem. Rev. 109 (2009) 3817;

(i) S. Díez-Gonzalez, N. Marion, S.P. Nolan, Chem. Rev. 109 (2009) 3612;

(j) G.C. Fortman, S.P. Nolan, Chem. Soc. Rev. 40 (2011) 5151.

[10] (a) J.-F. Lefebvre, M. Lo, D. Leclercq, S. Richeter, Chem. Commun. 47 (2011) 2976;

(b) J.-F. Lefebvre, M. Lo, J.-P. Gisselbrecht, O. Coulembier, S. Clément, S. Richeter, Chem. Eur. J 19 (2013) 15652.

[11] M. Abdelhameed, P.-L. Karsenti, A. Langlois, J.-F. Lefebvre, S. Richeter, R. Ruppert, P.D. Harvey, Chem. Eur. J 20 (2014) 12988.

[12] J.-F. Lefebvre, D. Leclercq, J.-P. Gisselbrecht, S. Richeter, Eur. J. Org. Chem. (2010) 1912.

[13] (a) T. Dröge, F. Glorius, Angew. Chem. Int. Ed. 49 (2010) 6940;

(b) D.J. Nelson, S.P. Nolan, Chem. Soc. Rev. 42 (2013) 6723.

[14] (a) W.A. Herrmann, M. Elison, J. Fischer, C. Köcher, G.R.J. Artus, Angew. Chem. Int. Ed. 34 (1995) 2371;

(b) W.A. Herrmann, M. Elison, J. Fischer, C. Köcher, G.R.J. Artus, Chem. Eur. J 2 (1996) 772.